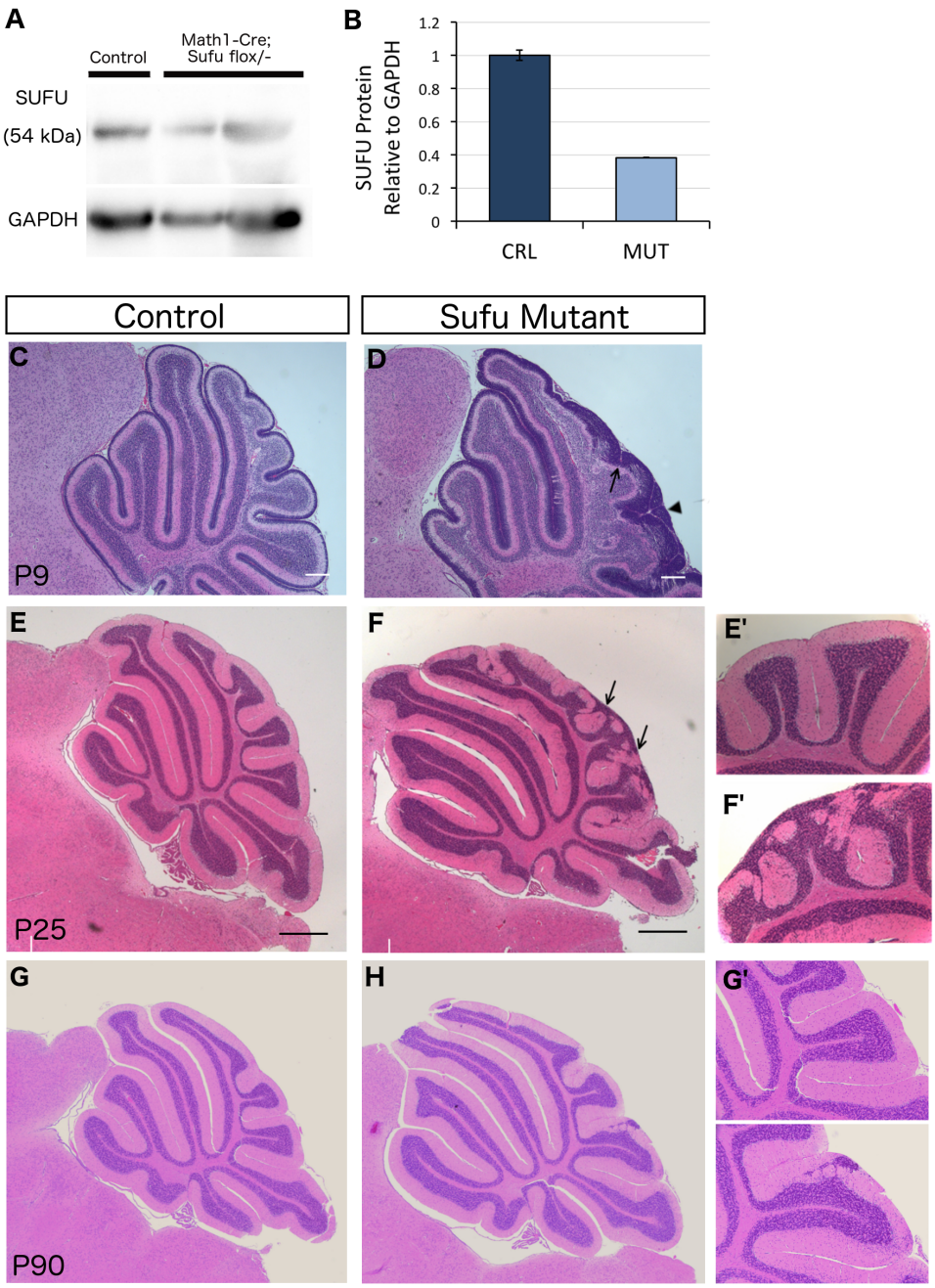

Figure S1 – Sufu deletion causes EGL hyperplasia and GC migration defects.

(A, B) Sufu protein is markedly in whole cerebellar lysate from P3 Sufu-mutant cerebella. (C-H) H&E stained sagittal sections from control and Sufu-mutant cerebella.The severely hyperplastic central lobules of P9 Sufu-mutant cerebella (D) display shallow fissures (arrow) and ectopic cell condensations (arrowhead) overlying the cerebellar surface. (E, F) The EGL is depleted by P25 in control (E), but not in Sufu-mutant cerebella (F) which displays ectopic EGL/ML cells and the absence of fissures between central lobules (arrows). (G, H) Ectopic ML cells and foliation abnormalities persist as late as P90. Scale bars: 200 μm.

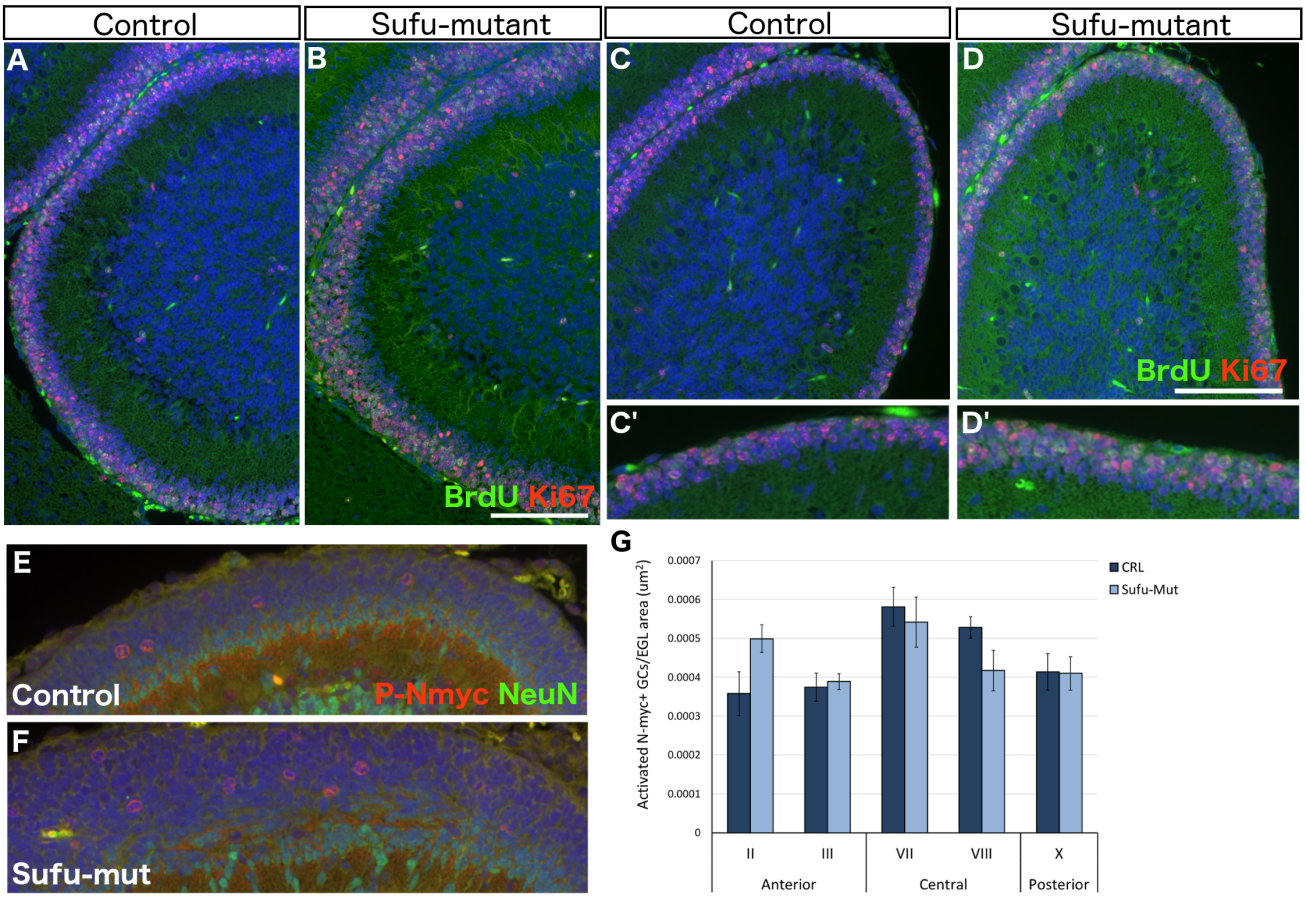

Figure S2 – GCP proliferation is increased across the Sufu-mutant cerebellum

(A-D) BrdU and Ki67 immunostaining in control (A, C) and Sufu-mutant (B, D) cerebella shown in representative anterior lobule (III) (A, B) and posterior lobule (X) (C, D). The EGL is noticeably thicker in Sufu-mutant lobules (B, D) and displays a greater number of BrdU+ (green) and Ki67+ (red) cells. Nuclei are labelled with DAPI (blue). (C', D') Higher magnification of boxed regions in C, D respectively. (E-F) Immunofluorescence staining at P8 detected phosphorylated Nmyc (P-Nmyc) (red) in outer EGL GCPs, which lack NeuN expression (green). (G) Quantitation of the number of P-Nmyc+ cells relative to total EGL area per lobule revealed no change in Sufu-mutants compared to control (n=3). Cell counts were compared in corresponding anterior (II, III), central (VII, VIII), and posterior (X) lobules.

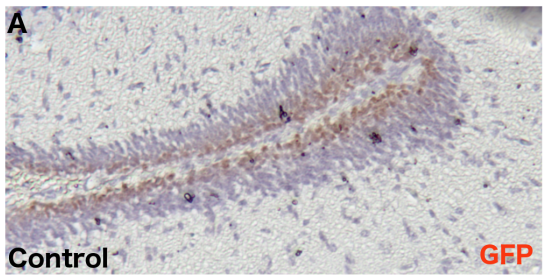

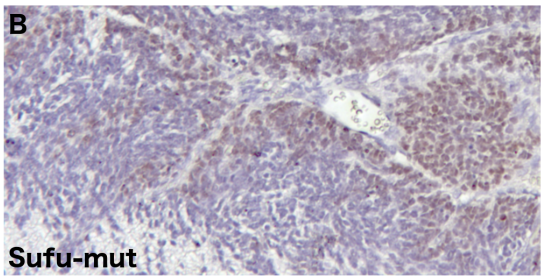

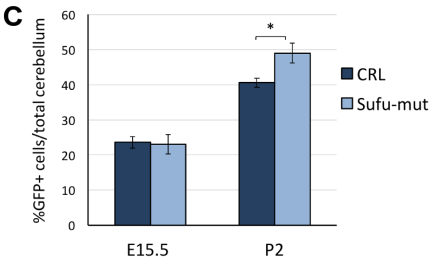

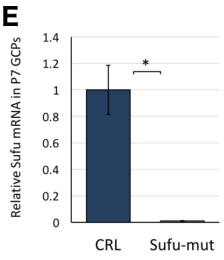

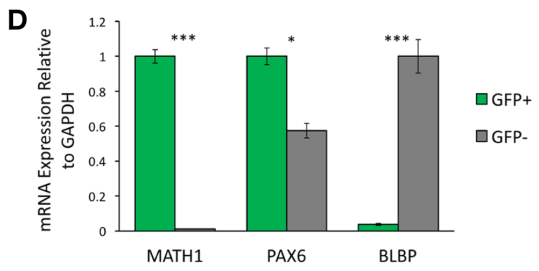

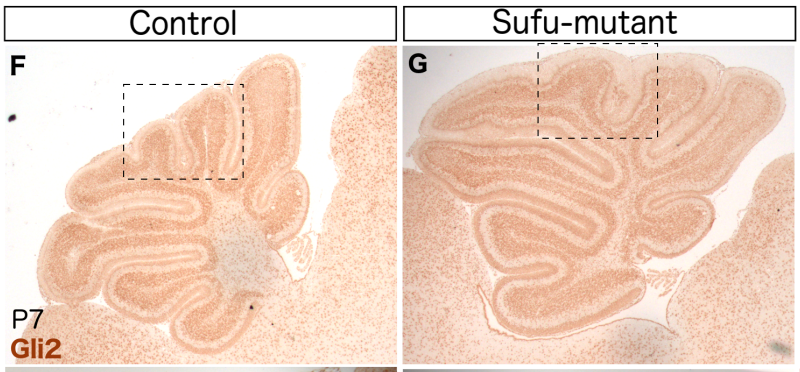

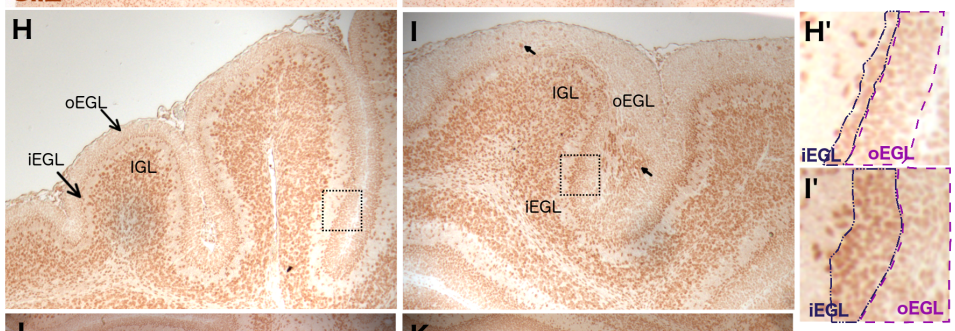

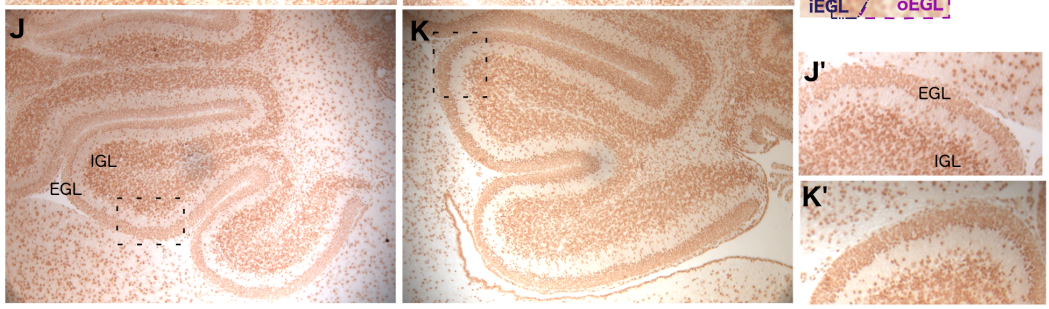

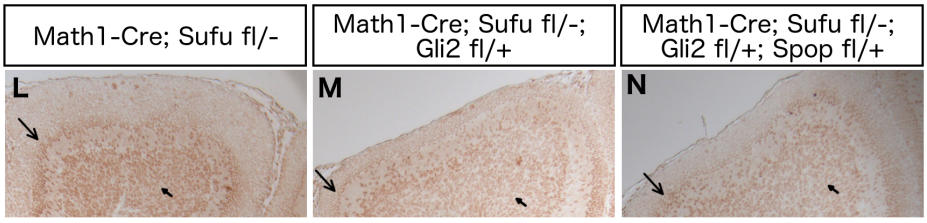

Figure S3 — Analysis of Shh signalling in Sufu-mutant cerebella and FACS-extracted GCPs.

(A, B) Math1-GFP expression labels cells in the outermost EGL, as shown by immunohistochemistry staining of control (A) and Sufu-mutant (B) cerebella. (C) Math1-GFP-expressing cells isolated from cell suspensions of control and Sufu-mutant cerebella. A significantly greater number of cells is isolated from Sufu-mutant cerebella at postnatal (n=13 crl, 7 Sufu-mut), but not embryonic (n=27 crl, 7 Sufu-mut) stages. (D) qRT-PCR analysis confirms absence of Sufu expression in FACS-purified cells from Sufu-mutant cerebella. (E) qRT-PCR analysis confirms enriched expression of GCP markers, Math1 and Pax6, and near absence of radial glial marker Blbp, in the GFP+ fraction extracted by FACS (n=3). Data are represented as mean ± SE. *P<0.05; **P<0.01; ***P<0.001. (F-N) Immunohistochemistry staining demonstrates Gli2 expression in the control (F) and Sufu-mutant cerebellum (G). Gli2 expression appears increased in the Sufu-mutant inner EGL (as compared to control) and in localized cell aggregates of the outer EGL (arrow, I). (I'-K') Higher magnification images of boxed regions in I-K. (L-N) Gli2 staining is reduced in the inner EGL is reduced after the deletion of Gli2 (M) as compared to the Sufu-mutant (L). Gli2 staining is then upregulated again (arrow) upon the deletion of ubiquitin ligase Spop which degrades Gli2 (N).

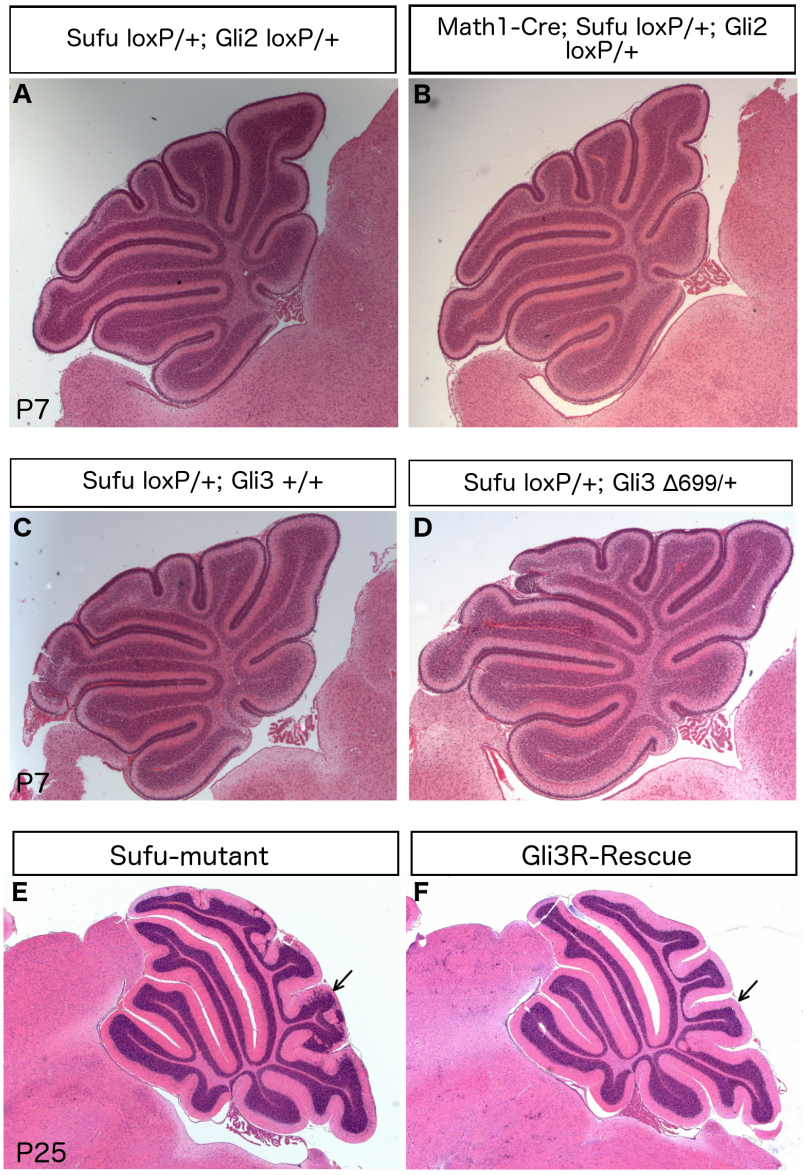

Figure S4 – Manipulation of Gli2 or Gli3R does not independently affect the EGL.

(A, B) Heterozygous deletion of Gli2 from GCPs in control cerebella (B) does not reduce or deplete the EGL, which appears comparable to wild-type (A). (C, D) Control cerebella expressing $Gli3^{\Delta 699}$ (D) appear indistinguishable from wild-type (C). (E, F) P25 cerebella demonstrate that Gli3R Rescue cerebella (F) lack ectopic cells which are observed to persist in the EGL/ML of Sufu-mutant cerebella at later stages (E).

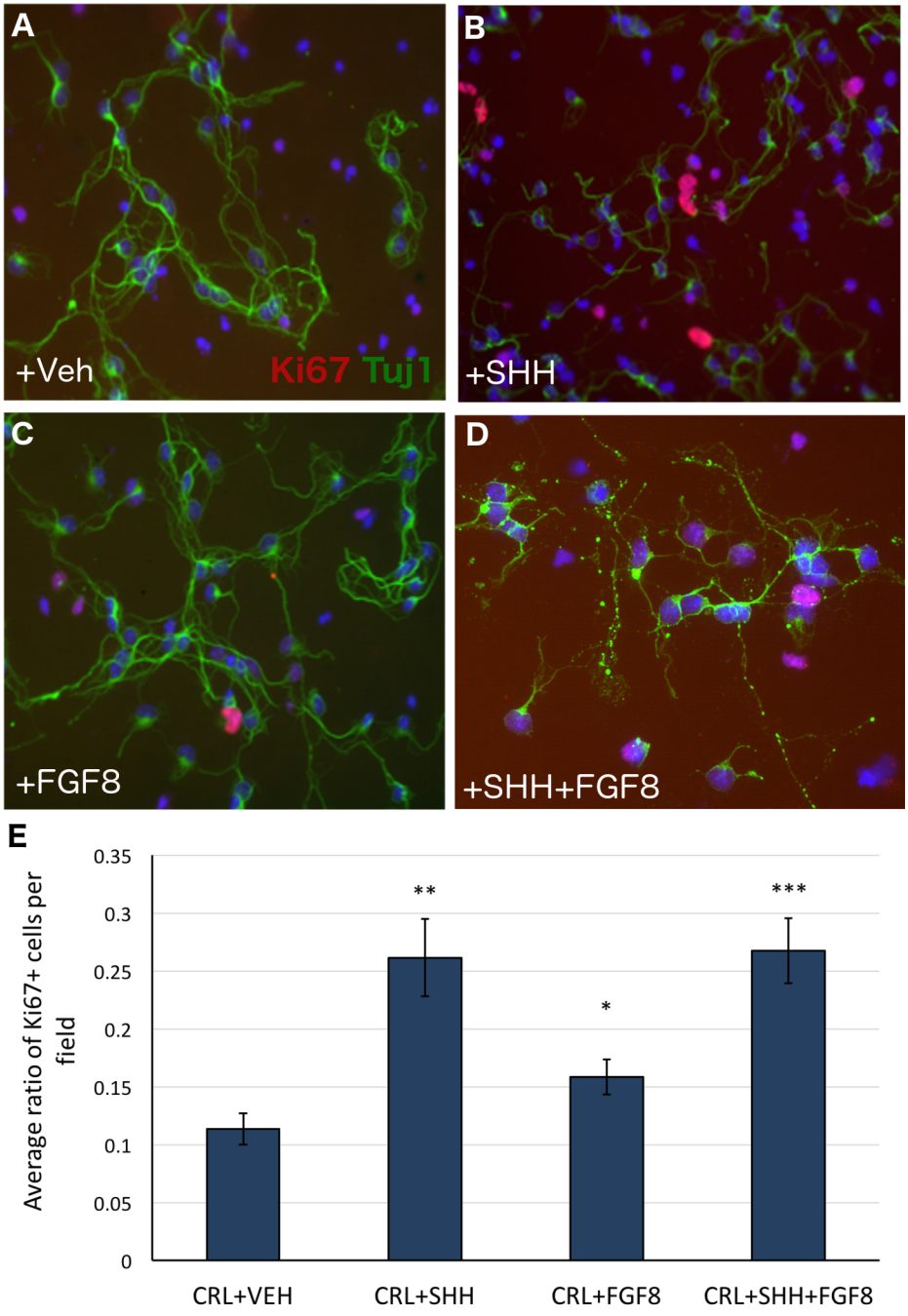

Figure S5 – Fgf8 stimulates GCP proliferation.

(A-D) FACS-purified wild-type GCPs cultured over 4 days with recombinant Shh, Fgf8b or vehicle (n=3 biological replicates/condition). Vehicle-treated GCPs generally lacked Ki67 expression (A), while Shh treatment robustly induced Ki67 (B). Elevated Ki67 expression was also observed in Fgf8-treated (C) and Shh+Fgf8 treated (D) GCPs. (E) Quantitation analyses confirmed that Fgf8 treatment significantly increases the ratio of Ki67+ cells relative to control. Two-tailed unpaired Student's t-test *P<0.05; **P<0.01; ***P<0.001.

Table S1 – List of differentially regulated genes detected by RNA-Seq, organized by fold-change in expression in P2 Sufu-mutant cerebella relative to control. Adjusted P value (P-adj) < 0.05.

Gene ID	Gene Name	P-adj Value	Fold Change
Fgf8	Fibroblast growth factor 8	9.92E-07	2.24
Plagl1	Pleiomorphic adenoma gene-like 1	3.32E-06	1.54
Chrnb4	cholinergic receptor, nicotinic, beta 4	9.04E-05	1.86
Crnmt1	Carnosine n-methyl transferase1	0.00054	1.79
Cldn2	Claudin-2	0.0013	1.74
Insm2	insulinoma-associated 2	0.0014	1.83
Car12	carbonic anhydrase 12	0.0031	1.69
Bmp5	bone morphogenetic protein 5	0.0033	1.67
Otx2	orthodenticle homeobox2	0.0033	1.50
Itga8	integrin, aplha 8	0.0035	1.58
Abca4	ATP-binding casette, subfamily A, member 4	0.0048	1.49
Defb11	Defensin beta 11	0.0048	1.75
Nmrk1	nicotinamide riboside kinase 1	0.0048	1.76
Sowaha	sosondowah ankyrin repeat domain family member A	0.0048	1.68
Kl	klotho	0.0053	1.65
Slc4a5	Solute carrier family 4, sodium bicarbonate cotransporter, member 5	0.0058	1.66
Trpv4	transient receptor potential cation channel, subfamily V, member 4	0.0077	1.63
Thrsp	thyroid hormone responsive	0.0084	1.69
Abcc9	ATP-binding cassette, subfamily C (CFTR/MR), member 9	0.0086	1.37
Frem1	Fras1 related extracellular matrix protein	0.0100	1.48
Ntf3	Neurotrophin 3	0.0162	1.62
Clic6	clhloride intracellular channel 6	0.0200	1.56
Adamts1	a disintegrin-like and metallopeptidase (reprolysin type) with thrombospondin type 1 motif, 1	0.0207	1.54
Cep162	centrosomal protein 162	0.0210	1.36
Zgrf1	zinc-finger GRF-type containing 1	0.0210	1.39

Wfikkn2	WAP, follistatin/kazal, immunoglobulin, kunitz and netrin domain containing 2	0.0213	1.56
Gmnc	geminin coiled-coil domain containing	0.0217	1.57
Fam84b	family with sequence similariy 84, member B	0.0234	1.44
Akna	AT-hook transcription factor	0.0241	1.49
Prtg	protogenin	0.0288	1.45
Vwa5b1	von Willebrand factor A domain containing 5B1	0.0333	1.47
Etv5	ets variant 5	0.0342	1.52
Prex2	phosphatidylinositol-3,4,5-trisphosphate-dependent Rac exchange factor 2	0.0351	1.47
Chrna3	cholinergic receptor, nicotinic, alpha polypeptide 3	0.0417	1.44
Ranbp17	RAN binding protein 17	0.0444	1.39
Baiap2l1	BAI1-associated protein 2-like 1	0.0449	1.50
Tle6	trasnducin-like enhancer of split 6	0.0479	1.52
Cdc14b	cell division cycle 14B	0.0493	1.41
Tmem72	transmembrane protein 72	0.0497	1.58
Sufu	suppressor of fused	0.00134	0.69
Neu4	neuraminidase/sialidase 4	0.00856	0.61
Nefl	neurofilament, light polypeptide	0.00936	0.65
Krt19	keratin 19	0.00972	0.59
Slc2a6	solute carrier family 2 (facilitated glucose transporter), member 6	0.00972	0.63
Htr3a	5-hydroxytryptamine (serotonin) receptor 3A	0.01005	0.59
Isl1	islet1/isl1 transcription factor	0.01399	0.59
Tppp3	tubulin polymerisation-promoting protein family member 3	0.02099	0.68
Fbxo2	F-box protein 2	0.02130	0.67
Calca	calcitonin/calcitonin-related polypeptide, alpha	0.03640	0.62
Ecel1	endothelin converting enzyme-like 1	0.04443	0.63